Simple and Accurate Procedure for Modeling Erbium-Doped Waveguide Amplifiers with High Concentration

M. V. D. Vermelho, Ulf Peschel, and J. Stewart Aitchison, *Member, IEEE, Member, OSA*

***Abstract*—In this paper, we present an accurate, fast, and easily implemented procedure for modeling erbium-doped waveguide amplifiers (EDWA's) with high concentration doping level. The model is shown to be in a very good agreement when compared with experimental results, and is used in a detailed analysis of a waveguide amplifier with 980-nm pumping.**

***Index Terms*—Erbium, integrated optoelectronics, laser amplifiers, luminescent devices, nonlinear systems, optical amplifiers, optoelectronic devices.**

I. Introduction

RECENT improvements of the performance of the available optical gain of erbium-doped waveguide amplifiers (EDWA's) have been maintaining the constant interest in this research field [1]–[5]. These integrated versions offer the prospect of combining passive and active components on the same substrate while producing compact and robust devices at lower cost than commercially available fiber-based versions. However, research on planar waveguide amplifiers has been encountering a serious obstacle in obtaining high optical gain. This is mainly due to the necessity of incorporating high erbium concentrations (usually more than ten times that of fiber amplifiers) to compensate for the short interaction length and higher losses of integrated waveguides. At high erbium ion concentrations, upconversion process considerably reduce the amplification and lasing performance of these devices [6]–[9].

Unlike optical fiber components, an integrated optical device has a fixed length which cannot be altered after fabrication, thus reducing the number of adjusting parameters to compensate for minor deviations. Therefore, accurate numerical models of integrated rare earth doped components, particularly at high concentration levels, are of great importance. A widely used numerical approach for modeling erbium doped waveguide amplifiers is a combination of the finite element method with a Runge–Kutta algorithm [2], [3]. In this method, the propagation equations of the pump, signal, and amplified spontaneous emission are numerically integrated using the Runge–Kutta method based on an iterative procedure. Population densities are computed in each finite element and at each step in the propagation direction, solving the rate equations numerically and using the normalized intensity profile previously obtained. This method has been shown to be very accurate. Unfortunately, it is not simply implemented on a computer and requires time-consuming calculations, making the optimization of more involved structures practically impossible.

In this paper, we present a new, very intuitive, and much simpler approach to model waveguide amplifiers with high erbium concentrations. The basic approximation used in the modeling is anchored on the small contribution of the nonlinear terms to the photon population densities. An assumption that is still valid in present laser and amplifier configurations. The model is tested against several experimental results and is shown to be in very good agreement.

II. The Amplifier Model

EDWA's pumped in the 980-nm absorption band have a very good performance with respect to optical gain, gain efficiency, and low noise level [7]. The large absorption cross section of the dopants, the complete absence of stimulated spontaneous emission and excited state absorption make this pump wavelength preferable [10]. Fig. 1 depicts the relevant energy levels for a highly doped erbium system. Following this diagram, the multilevel system of rate equations can be written as [11]

$$\frac{dN_1}{dt} = -(R + W_a)\cdot N_1 + (W_e + 1/\tau_{21})\cdot N_2 + C_{22}\cdot N_2^2 - C_{14}\cdot N_1\cdot N_4 + C_{33}\cdot N_3^2 \quad (1)$$

$$\frac{dN_2}{dt} = W_a\cdot N_1 - (W_e + 1/\tau_{21})\cdot N_2 + \frac{N_3}{\tau_{32}} - 2C_{22}\cdot N_2^2 + 2C_{14}\cdot N_1\cdot N_4 \quad (2)$$

$$\frac{dN_3}{dt} = R\cdot N_1 - \frac{N_3}{\tau_{32}} + \frac{N_4}{\tau_{43}} - 2C_{33}\cdot N_3^2 \quad (3)$$

$$\frac{dN_4}{dt} = -\frac{N_4}{\tau_{43}} + C_{22}\cdot N_2^2 - C_{14}\cdot N_1\cdot N_4 + C_{33}\cdot N_3^2 \quad (4)$$

where R, W_a, and W_e are the pump, stimulated absorption and emission transition rates, respectively, defined by

$$R \equiv R(x,y,z) = \frac{\sigma_{\mathrm{pa}}\cdot I_p(x,y,z)}{h\cdot v_p} \quad (5)$$

Manuscript received December 12, 1998; revised July 30, 1999.

The authors are with the Department of Electronics and Electrical Engineering, University of Glasgow, Glasgow G12 8QQ, U.K. (e-mail: m.vermelho@elec.gla.ac.uk).

Publisher Item Identifier S 0733-8724(00)02296-9.

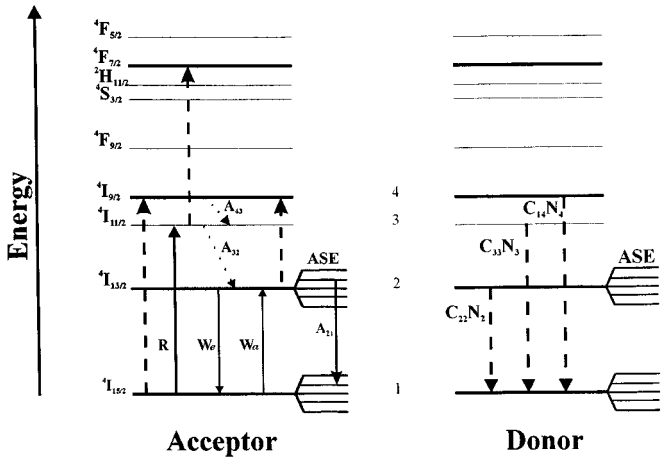

Fig. 1. Relevant energy levels for a highly doped erbium system. The cross-relaxation and upconversion transitions between two erbium ions are represented by dashed arrows in both graphs.

$$W_a \equiv W_a(x,y,z) = \frac{\sigma_{\rm sa}(\upsilon_s)\cdot I_s(x,y,z)}{h\cdot \upsilon_s} + \sum_{i=1}^{N} \frac{\sigma_{\rm sa}(\upsilon_i)}{h\cdot \upsilon_i}[I^{+}_{\rm ASE}(x,y,z) + I^{-}_{\rm ASE}(x,y,z)] \quad (6)$$

$$W_e \equiv W_e(x,y,z) = \frac{\sigma_{\rm se}(\upsilon_s)\cdot I_s(x,y,z)}{h\cdot \upsilon_s} + \sum_{i=1}^{N} \frac{\sigma_{\rm se}(\upsilon_i)}{h\cdot \upsilon_i}\left[I^{+}_{\rm ASE}(x,y,z) + I^{-}_{\rm ASE}(x,y,z)\right] \quad (7)$$

where $I_p(x,y,z), I_s(x,y,z)$, and $I^{\pm}_{\rm ASE}(x,y,z)$ are the pump, signal, and amplified spontaneous emission intensities respectively. $\sigma_{\rm pa}, \sigma_{\rm sa}(\nu_i)$, and $\sigma_{\rm se}(\nu_i)$ are the cross sections for the pump, the signal and for the spontaneous emission respectively. τ_{21} is the fluorescence lifetime of the metastable ($^4I_{13/2}$) level, and $1/\tau_{32}$ and $1/\tau_{43}$ accounts for the multiphonon nonradiative relaxations $^4I_{9/2} \rightarrow {}^4I_{11/2}$ and $^4I_{11/2} \rightarrow {}^4I_{13/2}$, respectively. The population density of the level $^4F_{7/2}$ is assumed negligible because of the very short lifetime of this state.

The upconversion coefficient C_{22} has been measured indirectly from spectroscopic data. The measured values are of the order of $10^{-22} - 10^{-23}$m^3/s [23]. Unfortunately, the other coupling constants (C_{33} and C_{14}) have not been determined and only rough order-of-magnitude estimates are available. This may be a significant source of uncertainties, which have to be taken into account when high doping level and ion-ion interactions are considered. The C_{33} and C_{14} coefficients are expected to be smaller than C_{22} due to their indirect dependence on the population level as was experimentally demonstrated [6].

In the steady state, the relevant population densities N_1, N_2, N_3, and N_4 of the respective levels $^4I_{15/2}, {}^4I_{13/2}, {}^4I_{11/2}$, and $^4I_{9/2}$, are computed by setting each rate equation as zero and using the photon conservation law:

$$N_0(x,y) = N_1(x,y,z) + N_2(x,y,z) + N_3(x,y,z) + N_4(x,y,z). \quad (8)$$

The total erbium concentration N_0 is assumed to be homogeneously distributed along the direction of propagation.

Because the induced index changes are very small (<0.02), we may still assume that the shapes of the individual waveguide modes are conserved, while their amplitudes evolve during propagation along the waveguide. In what follows, we assume monomode operation.

The evolution of the pump, signal and amplified spontaneous emission (ASE) powers along the waveguide length (L) are consequently described by the following integro-differential equations:

$$\frac{dp(z)}{dz} = -\gamma_{\rm pa}(z)\cdot p(z) - \alpha_p \cdot p(z) \quad (9)$$

$$\frac{ds(z,\upsilon_s)}{dz} = [\gamma_{\rm se}(z,\upsilon_s) - \gamma_{\rm sa}(z,\upsilon_s)]\cdot s(z,\upsilon_s) - \alpha_s \cdot s(z,\upsilon_s) \quad (10)$$

$$\frac{ds^{\pm}_{\rm ASE}(z,\upsilon_i)}{dz} = \pm[\gamma_{\rm se}(z,\upsilon_i) - \gamma_{\rm sa}(z,\upsilon_i) \mp \alpha_s] \cdot s^{\pm}_{\rm ASE}(z,\upsilon_s) \pm m\cdot h\cdot \upsilon_i \cdot \Delta\upsilon_i \cdot \gamma_{\rm se}(z,\upsilon_i). \quad (11)$$

The absorption and emission coefficients $\gamma_{\rm pa}, \gamma_{\rm se}$, and $\gamma_{\rm sa}$ in (9)–(11) are spatial overlap integrals expressions involving the normalized pump and signal energy density profile, $\psi_p(x,y)$ and $\psi_s(x,y)$, and the population levels are given by

$$\gamma_{\rm pa}(z) = \iint_{\rm core} \sigma_{\rm pa}\cdot N_1(x,y,z)\cdot \psi_p(x,y)\cdot dA \quad (12)$$

$$\gamma_{\rm sa}(z,\upsilon_i) = \iint_{\rm core} \sigma_{\rm sa}(\upsilon_i)\cdot N_1(x,y,z)\cdot \psi_s(x,y)\cdot dA \quad (13)$$

$$\gamma_{\rm se}(z,\upsilon_i) = \iint_{\rm core} \sigma_{\rm se}(\upsilon_i)\cdot N_2(x,y,z)\cdot \psi_s(x,y)\cdot dA. \quad (14)$$

The intensity profile $\psi_s(x,y)$, is assumed to coincide for all the signal and the ASE fields.

Background losses are represented using α_p, and α_s for pump and signal frequencies, respectively. The ASE spectrum is computed, for each guided mode m, at the signal wavelength, sampling the emission cross-section profile spectra of the laser transition in a set of N frequency slots with equal width $\Delta\nu_i$ centred at the frequency ν_i [12]. The set of $2\cdot(N+1)$ nonlinear integro-differential equations is solved, subject to the following boundary conditions, $p(0) = P_p(0)$, $s(0) = P_s(0,\nu_s) = P_s(0)$, and to $s^{+}_{\rm ASE}(0,\upsilon_i) = s^{-}_{\rm ASE}(L,\upsilon_i) = 0$ $(i = 1,\ldots,N)$.

III. Modeling of Low Rare-Earth Concentrations

In the case of fiber-based optical devices, where the erbium concentrations is low, the modeling is quite easy [13]–[16]. The nonlinear terms in (1)–(4) can be dropped $(C_{ij} = 0)$ and the continuous-wave (CW) population equations are linear with respect to the doping concentration. Consequently the two laser levels considered in the population inversion process can be expressed as a function of the pump and signal intensities analytically and the resulting expressions can be inserted into the overlap integrals (12)–(14). Therefore, the whole numerical procedure simplifies considerably.

IV. Modeling of High Doping Level EDWA

In the case of integrated waveguide amplifiers, or lasers, the erbium concentrations are usually high to neglect the nonlinear contributions in (1)–(4). Although there is no simple way to relate the population densities to the intensities in the waveguide, we may still benefit from the procedure demonstrated above for low erbium concentrations. The basic approximation used in the modeling is anchored on the overall small contribution of these nonlinear terms.

In what follows, we briefly estimate the influence of the nonlinear terms which manifest itself in the presence of the population densities N_3 and N_4. Considering the levels with energy below 21 000 cm^{-1}, which correspond to the $^4\text{F}_{7/2}$ level, the largest multiphonon relaxations are due to the following energy gaps: $^4S_{3/2} \rightarrow {}^4F_{9/2}$, $^4F_{9/2} \rightarrow {}^4I_{9/2}$, and $^4I_{11/2} \rightarrow {}^4I_{13/2}$; corresponding to the energy gaps of $\Delta E_1 \approx 2800\ \text{cm}^{-1}$, $\Delta E_2 \approx 2600\ \text{cm}^{-1}$, $\Delta E_3 \approx 3300\ \text{cm}^{-1}$, respectively [21].

Now we study the contribution of the nonradiative transition probabilities and their influence on the population of the main Stark levels involved. Nonradiative decay rates W_{nr} are inversely proportional to the exponential of the energy gap separating the two levels involved. The multiphonon nonradiative decay rates can be determined by: $W_{\text{nr}} = C \cdot [n(T) + 1]^p \cdot e^{-(\alpha \cdot \Delta E)}$ [21]. Where C and α are host-dependent parameters, assumed to be $5.4 \times 10^{12}\ \text{s}^{-1}$ and 4.7×10^{-3} cm respectively, ΔE correspond to the energy gap, p is the number of phonon required to bridge the gap, and $n(T)$ is the Bosen-Einstein occupation number of the effective phonon number, $n(T) = [e^{(h\nu/kT)} - 1]^{-1}$. The phonon energy is $h \cdot \nu = 1200$ cm^{-1} for the glass studied. The nonradiative transition rates are $W_{\text{nr1}} \approx 1.1 \times 10^7\ \text{s}^{-1}$, $W_{\text{nr2}} \approx 2.7 \times 10^7\ \text{s}^{-1}$, $W_{\text{nr3}} \approx 1.0 \times 10^6$ s^{-1} respectively [22]. As it is observed, even the slowest transition rate, W_{nr3}, is three order-of-magnitude faster than the metastable level with a lifetime of approximately 5 ms for phosphosilicate glasses. Thus, at normal pump power (~100 mW), and typical experimental parameters values ($\sigma_{\text{ap}} \sim 2.0 \times 10^{-25}$ m^2, $\lambda_p = 980$ nm, $n \sim 1.5$) [6] the pump transition rate, $R = (\sigma_{\text{ap}}/h\nu_p) \cdot I_p \approx 42 \cdot I_p\ \text{s}^{-1}$, is still two orders of magnitude smaller than the nonradiative decay rate ($W_{\text{nr}} \sim 250R$) and the population of the Stark levels above $^4I_{13/2}$ remains small. Therefore, the linear equations involving levels one and two only can be used, as a first approximation, to describe the whole laser system.

We assume all the constants of the nonlinear terms to be equal to C_{22} $(C = C_{ij})$. This represents the strongest influence of the nonlinear terms and therefore the less favorable situation to optimize the optical gain of an amplifier

$$\begin{aligned} \mp (R + W_\alpha) \cdot N_1 \pm (W_e + 1/\tau_{21}) \cdot N_2 \\ \mp C \cdot \left(N_2^2 + N_3^2 - N_1 \cdot N_4\right) = 0 \end{aligned} \tag{15}$$

where the upper signals are related to the N_1 dynamic behavior and the lower to the N_2.

Applying experimental parameters to (15), the contribution of the nonlinear term of these equations are estimated to be approximately one to three orders of magnitude smaller than the individual linear terms.

Therefore, we may assume that the spatial distribution of the levels 1 and 2 to be still the same as in the linear case and that the nonlinear terms introduce a small correction only

$$\tilde{N}_i(x, y, z) \approx N_i^L(x, y, z) \left[1 + \Delta_i^{NL}(Z)\right]. \tag{16}$$

This assumption is the basic approximation of our approach. In (16) $N_i^L(x, y, z)$ are the explicit expressions for the populations N_1 and N_2 defined for the low concentration devices, i.e., setting all the nonlinear upconversion and cross-relaxation terms equal zero, and $\Delta_i^{\text{NL}}(z)$ are small corrections, which account for the nonlinear contributions due to the cross-relaxation processes. The nonlinear factors are calculated as

$$\Delta_i^{\text{NL}}(z) = \frac{N_i^{\text{NL}}(x, y, z)}{N_i^L(x, y, z)} - 1 \tag{17}$$

where $N_i^L(x, y, z)$ and $N_i^{\text{NL}}(x, y, z)$ are the population densities of the levels i in the absence and presence of cross-relax-

TABLE I
Spectroscopic Parameters for the Er^{3+}-doped P_2O_5-SiO_2 Planar Waveguides Used in the Modeling

Description	Parameter Value (Unit)
Pump wavelength, λ_p	980 nm
Signal wavelength, λ_s	1533 nm
Pump peak cross-section, σ_{ap}	$(2.0\text{-}3.2)\cdot 10^{-25}$ m^2
Signal peak cross section, $\sigma_{sa} = \sigma_{se}$	$(5.6\text{-}9.1)\cdot 10^{-25}$ m^2
Cladding refractive index	1.51164
Radiative lifetime, τ_{21}	(8.0-12.5) ms
Nonradiative transition rates, A_{32} , A_{43}	$5\cdot 10^4\ \text{s}^{-1}$, $4\cdot 10^4\ \text{s}^{-1}$
Upconversion coefficients, $C_{22} = C_{33} = C_{14}$	$(-6.40 + 18.00\cdot wp)\cdot 10^{-24}$ m^3/s

TABLE II
Summary of the Variable Parameters for Each Amplifier Analysed. The Parameters Listed Are Respectively the Waveguide Length, the Rectangular Waveguide Cross-Section, the Measured Scattering Losses, the Erbium Concentration, and the Refractive Index Difference Between Cladding and Core Layers

	Length (cm)	Core dimensions (μm)	Loss (dB/cm)	Concentr. (wt%)	Δn (%)	Reference
Figure 3	7.5	11 x 8	0.17	0.48	1.6	24
Figure 4	19.4	8 x 7	0.07	0.54	1.2	25

ation, respectively. $N_i^{\mathrm{NL}}(x,y,z)$ are obtained through the numerical solutions of the system of equations.

We will check the accuracy of this approximation by comparing the calculations with experimental results obtained for well-examined waveguide amplifiers [24], [25]. All the input data, obtained from the referenced papers, and used for modeling are shown in Tables I and II. Table I contains a list of common parameters for the two amplifiers, and Table II are the specific parameters related to each particular waveguide.

For a gain system such as erbium around 1500 nm, not only the stimulated emission but also the absorption cross section play an important role in determining the performance. As generally, the local crystalline structure affects the cross section of the rare-earth ion, however, only the host has the strongest effect upon their magnitude and shape [10]. Due to the spectral shape invariance of the absorption and emission cross-sections, a typical spectra obtained from spectroscopic measurements, depicted in Fig. 2 [34], were used for all simulations. For each amplifier, depending on the concentration level, a peak value was adopted as an adjustable parameter. Choosing slightly different lifetimes compensated minor deviations between theoretical and experimental results.

The upconversion coefficients were assumed to be an increasing linear function of the rare-earth concentration as proposed in [23]. Forward and backward amplified spontaneous emission has been spectrally resolved by using 100 frequency slots from 1450 to 1650 nm. The input signal to be amplified was considered as $P_s(0) = 1\ \mu$W for all simulations.

The open squares shown in Fig. 3 correspond to experimental results of a waveguide amplifier with a core of erbium doped phosphosilicate glass formed by PECVD. The undercladding and cladding were formed by flame hydrolysis deposition (FHD), on Si substrate. Solid circles show the results of this model using the approximation equation (16) introduced in the overlap integrals equations (12)–(14). A reported maximum net gain of 5 dB pumped at 420 mW, is very close to the 4.9 dB at the same pump power obtained theoretically. An excellent agreement of the 0 dB gain threshold was achieved between the measured 23 mW and the 25 mW calculated. Within the whole span of the reported pump power, less than 5% difference between experimental and theoretical results was observed.

A final test of the validity of the model is performed through a comparison of the results of the amplifier gain reported in the Fig. 4(a) to Fig. 4(c). Measurements shown in Fig. 4(b), reported in reference the best result, a net gain of 13.7 dB in a 19.4 cm long waveguide pumped at 500 mW [27]. Under the same situation the model calculated a 13.55 dB net gain. The influence of uniform and pair induced upconversion mechanisms are also considered. Di Pasquale et al. [26], modeling these two nonlinear mechanisms in the same waveguide structure, proposed the inclusion of a linear concentration function for the coefficients, as reported in Table I, and to include a moderate amount of clustering to calculate the amplifier gain. Both were considered in the present modeling which shows a good fitting to the experimental data reported in Fig. 4(c).

Now we try to optimize the configuration shown in Fig. 3. The gain of high concentration erbium doped waveguide amplifier can be improved by modeling geometrical parameters

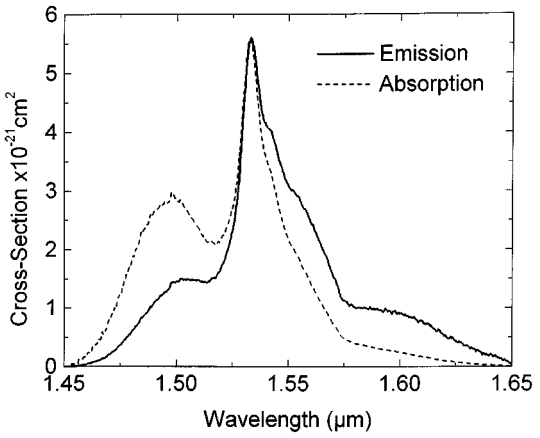

Fig. 2. Typical emission and absorption cross sections for an erbium-doped phosphosilicate glass system (SiO_2-P_2O_5) formed by flame hydrolysis deposition [34].

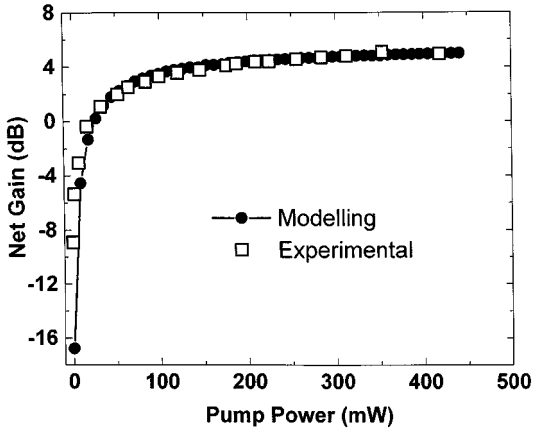

Fig. 3. Comparison of experimental result (open squares) [23] and calculated (solid circles) of the amplifier single pass gain dependence versus pump power [Ps$(0) = 1\ \mu$W].

such as core cross-section, waveguide length, or by improving fabrication processes eg. increasing erbium concentration, and reducing background losses, or finally by operational condition like pump power regime. Among them, background losses are the major reason for a decrease of the amplifier performance. It results mainly from the combination of internal scattering, surface scattering, Rayleigh scattering [27], however, the major role is due to the local deformations at lateral walls during etching process [28]–[30]. However, background loss is not strictly a design characteristic, but rather a consequence of the buried channel waveguides fabrication process, and improving the fabrication process it can be reduced [31], [32].

This waveguide characterization starts choosing feasible refractive index difference and background losses. Experimental values of $\Delta n = 1.0\%$, for the refractive index, and $\alpha_{Lp} = 9.13$ dB/m and $\alpha_{Ls} = 7.18$ dB/m [33], for the background losses near the pump and signal wavelengths, respectively, are already reported.

The first geometrical parameter to be optimized to increase the gain is the waveguide cross section. Fig. 5 depicts a simulation result for a squared cross sectional (A) waveguide. These

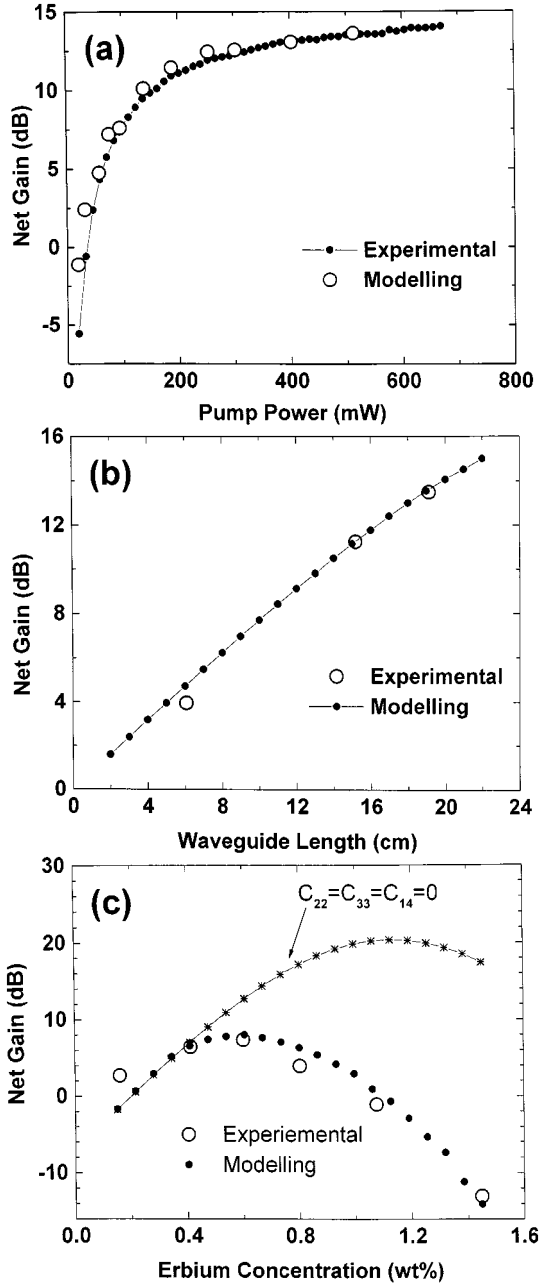

Fig. 4. (a) Comparison of experimental result (solid circles) [24] and calculated (open circles) of the amplifier single pass gain dependence versus pump power [Ps$(0) = 1$ mW]. (b) Experimental (open circles) and theoretical (solid circles) single pass net gain characteristic versus waveguide length [Pp$(0) = 500$ mW, Ps$(0) = 1$ μW]. (c) Dependence of the single pass net gain on erbium concentration [Pp$(0) = 100$ mW, Ps$(0) = 1$ μW]. The curve represented by "stars" correspond to the simulation considering a linear system of rate equations [$C_{i,j} = 0$].

results were performed in two distinct situations. First, represented by open squares, pump and signal were forced to propagate along the waveguide in the fundamental propagation mode despite the cross section dimensions. During the second simulation, shown as "stars" in the same graph, the program is allowed to change to the highest propagation modes as the cross section increase. The gaps shown in the second calculated maximum net gain correspond to these modes propagation change. It is observed that, independently of the propagation condition, there is a maximum net gain within the monomode propagation

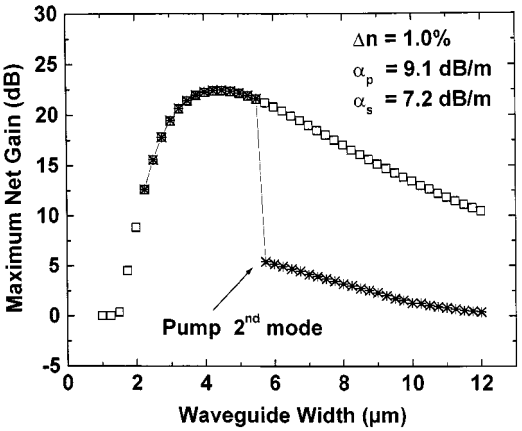

Fig. 5. Maximum single pass net gain versus waveguide squared cross section [Pp$(0) = 100$ mW, Ps$(0) = 1$ μW].

regime, where the overlap integral reaches a maximum. For this waveguide configuration this maximum occurs when the cross section correspond to a square with 4.5 μm $\times$ 4.5 μm sides.

This simulation was carried out considering feasible waveguide length and erbium ions incorporation into the glass fabricated by FHD. Long waveguides presuppose an increasing in the background losses due to the nonuniform walls resulting from the etch process. Furthermore, the spiral path necessary to achieve long waveguide length on a small substrate adds a considerable amount of bend loss. The doping level is limited by the solubility of the rare earth chlorides for a solution doping technique. Solidification of delivered solutions into the torch, before the flame, results in irreversible surface damaging on the deposited sample and is a limitation for the aerosol doping technique.

In Fig. 6(a), we show the net gain as a function of waveguide length and erbium concentration. In this graph, the region of negative gain, for long waveguide length and high rare earth doping levels, are intentionally set equal zero after simulation. It is observed a maximum peak gain region which correspond to an optimum waveguide amplifier configuration. A better visualization of this peak region is seen in Fig. 6(b), which corresponds to the gain contour curve diagram for Fig. 6(a).

The locus of maximum gain for each concentration, and the correspondent waveguide length necessary to achieve it, is plotted in the Fig. 6(c). The highest gain of 25.84 dB is predicted for a 22.74-cm-long waveguide with an erbium–ion concentration of 0.91 wt%. Fig. 7(a) depicts the amplifier optimizations as a function of launched pump power defining the region of saturation regime. Fig. 7(b) shows the two regime of an amplifier as a function of the input signal. The possibility of evaluate the ASE contribution on the amplifier performance, as a forward ASE spectrum shown in Fig. 7(c), is useful for a small signal regime design to evaluate signal-to-noise ratio (SNR) in an amplifier.

V. Computing Time Evaluations

It is worthwhile to comment on the computation time required during some evaluations. While maintaining a fixed precision in the propagation subroutine, it was observed a linear variation between the run time simulations and the

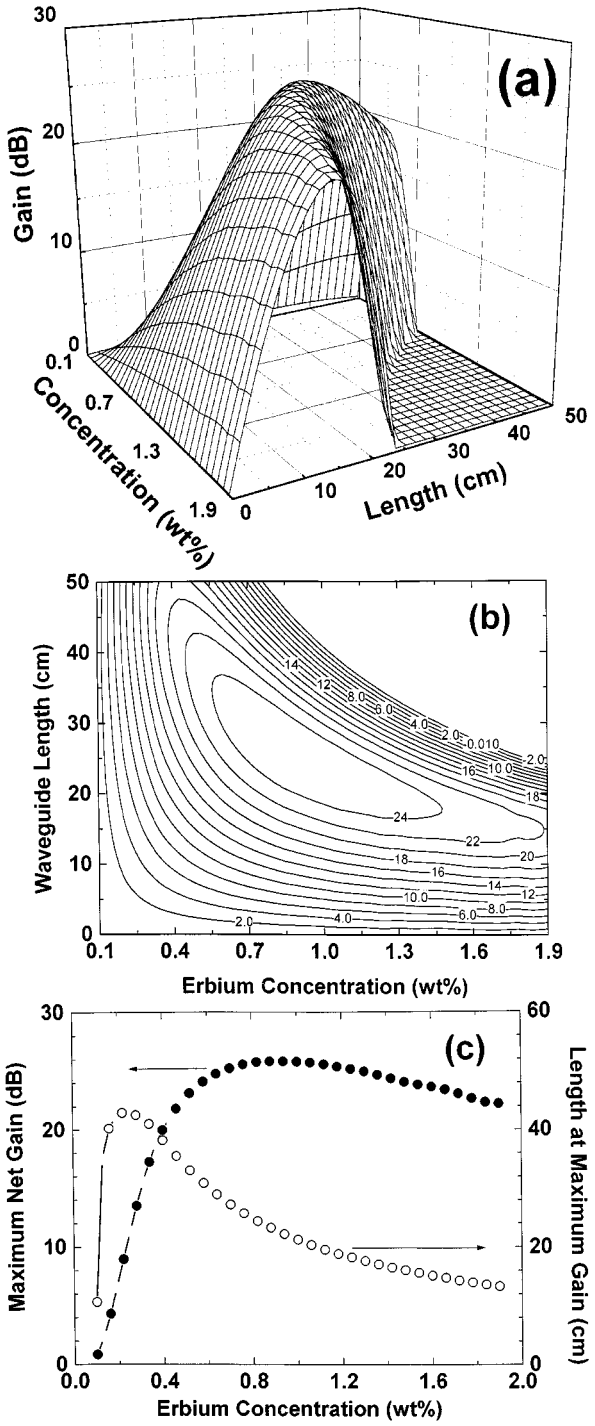

Fig. 6. (a) Surface plot of the amplifier gain as a function of the erbium concentration and waveguide length [Pp$(0) = 100$ mW, Ps$(0) = 1$ μW]. (b) Contour plot of Fig. 6(a). (c) Locus of the maximum gains of the contour plot.

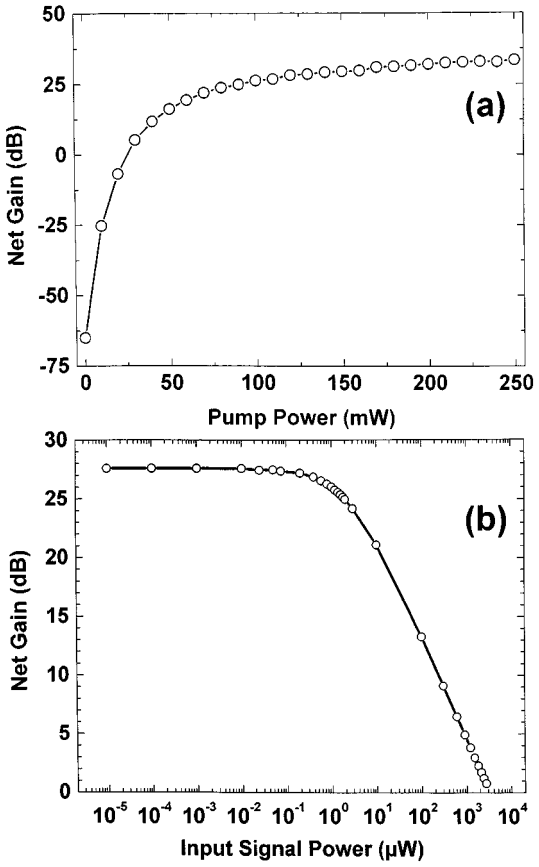

Fig. 7. (a) Optimized amplified gain characteristic versus pump power [core 4.5×4.5 μm^2, $L_G = 22.74$ cm, $N_{\rm cr} = 0.91$ wt%, Ps$(0) = 1$ μW]. (b) Amplifier net gain as a function of the input signal power [Pp$(0) = 100$ mW]. (c) Output ASE forward spectrum [Pp$(0) = 40$ mW, Ps$(0) = 1$ μW].

number of equations used to evaluate the amplified spontaneous emission (ASE). Propagation considering only two differential equations, no ASE, takes approximately 12 s. Whereas, for 400 ASE differential equations it took about 100 s for the same distance propagated. This run time increasing represented a variation of less than $\pm 2\%$ in calculated gain, as compared to the experimental measured at the same pump power. This variation in the calculated gain is much less than the uncertainties in some measured experimental parameters necessary as input data, such as cross section and lifetime. The same calculations were also performed for the saturated regime to minimize the influence of the ASE on the net gain. As the precision in the adjustable-step size subroutine is a determinate factor of the run time, it too was measured. An increase of the precision from 10^{-5} to 10^{-9} resulted in increase in the run time from 12 s to 110 s, whereas the calculated gain was not altered for more than 0.01%. This small influence of the precision on the calculated gain is true for relative low concentrations ($\sim$0.50 wt%), when the gain varies smoothly along the waveguide. For a heavily doped material ($\sim$1.50 wt%) a similar variation of precision can result in a difference of up to 7% in the gain. However, smaller step sizes and accuracy does not have a linear relation. Less than 1.5% of improvement in the gain, against the 12 minutes run time, is obtained if the precision is altered from 10^{-9} to 10^{-11}. All these results came from simulation programs written in FORTRAN-77 running on an IBM/PC—Pentium with 100 MHz clock rate.

Forward and backward amplified spontaneous emissions were sampled in 100 frequency slots each. Pump, signal, and ASE, as a set of 202 coupled differential equation, are solved by numerical integration through the waveguide in approximately

115 s, showing the validity of this tool to design erbium-doped waveguide amplifiers.

VI. Conclusion

After the preceding experimental and theoretical comparisons, the approximation proposed and introduced in the present modeling, shows to be suitable to analyze and optimize high concentration erbium-doped waveguide amplifier. This high accuracy is not only attributed to the small contribution of the nonlinear terms of the population equations, but also to the unique approximation used to solve the problem. The amplifier model was tested against two different well-known waveguide amplifiers. Within the inaccuracy of any missing input data, all calculations have shown very good agreement with the respective experimental results. Besides, very simple and fast computer programs can be generated using this new approach. For that reason, become a simple task to deal with hundreds of differential equations at the same time, and the degradation of noise figure can be estimated through the amplified spontaneous emission prediction. One of the great achievement of this calculations is the possibility of, after some implementation in the computer program, predict and optimize CW operation of high concentration erbium doped waveguide laser. A similar code has been implemented to model Er^{3+}/Yb^{3+} waveguide laser system.

Acknowledgment

M. V. D. Vermelho would like to thank the Brazilian Agency CNPq (Conselho Nacional de Desenvolvimento Cientfóico e Tecnológico) for his graduate studentship sponsoring.

References

[1] T. Rasmussen, A. Bjarklev, J. H. Povlsen, O. Lumholt, and K. Rottwitt, "Numerical modeling of an integrated erbium-doped glass laser," *Fiber Integr. Opt.*, vol. 10, pp. 239–243, Dec. 1991.

[2] F. Di Pasquale and M. Zoboli, "Analysis of erbium-doped waveguide amplifiers by a full-vectorial finite-element method," *J. Lightwave Technol.*, vol. 11, pp. 1565–1574, Oct. 1993.

[3] F. Di Pasquale, M. Zoboli, M. Federighi, and I. Massarek, "Finite-element modeling of silica waveguide amplifiers with high erbium concentration," *IEEE J. Quantum Electron.*, vol. 30, pp. 1277–1282, May 1994.

[4] O. Lumholt, A. Bjarklev, T. Rasmussen, and C. Lester, "Rare earth-doped integrated glass components: Modeling and optimization," *J. Lightwave Technol.*, vol. 13, pp. 275–282, Feb. 1995.

[5] P. Torres and A. M. Guzman, "Complex finit-element method applied to the analysis of optical waveguide amplifiers," *J. Lightwave Technol.*, vol. 15, pp. 546–550, Mar. 1997.

[6] H. Masuda, A. Tanaka, and K. Aida, "Modeling the gain degenaration of high concentration erbium-doped fiber amplifiers by introducing inhomogeneous cooperative up-conversion," *J. Lightwave Technol.*, vol. 10, pp. 1789–1799, Dec. 1992.

[7] Y. Kimura and M. Nakazawa, "Gain characteristics of erbium-doped fiber amplifiers with high erbium concentration," *Jpn. J. Appl. Phys.: Part 1*, vol. 32, pp. 1120–1125, Mar. 1993.

[8] M. Federighi, I. Massarek, and P. F. Trwoga, "Optical amplification in thin optical waveguide with high erbium concentration," *IEEE Photon. Technol. Lett.*, vol. 5, pp. 227–229, Feb. 1993.

[9] J. Thogersen, N. Bjerre, and J. Mark, "Multiphonon absorption and cooperative upconversion excitation in Er^{3+}-doped fibers," *Opt. Lett.*, vol. 18, pp. 197–199, Feb. 1993.

[10] W. J. Miniscalco, "Erbium-doped glasses for fiber amplifiers at 1500 nm," *J. Lightwave Technol.*, vol. 9, pp. 234–250, Feb. 1991.

[11] W. Q. Shi, M. Bass, and M. Birnbaum, "Effects of energy transfer among Er^{3+} ions on the fluorescence decay and lasing properties of heavily doped $Er:Y_3Al_5O_{12}$," *J. Opt. Soc. Amer. B*, vol. 7, pp. 1456–1462, Aug. 1990.

[12] M. Desurvire and J. R. Simpson, "Amplification of spontaneous emission in erbium-doped single-mode fibers," *J. Lightwave Technol.*, vol. 7, pp. 835–845, May 1989.

[13] M. J. F. Digonnet and C. J. Gaeta, "Theoretical analysis of optical fiber laser amplifiers and oscillators," *Appl. Opt.*, vol. 24, pp. 333–342, Feb. 1985.

[14] J. R. Armitage, "Three-level fiber laser: A theoretical model," *Appl. Opt.*, vol. 27, pp. 4831–4836, Dec. 1988.

[15] B. Pedersen, A. Bjarklev, J. H. Povlsen, K. Dybdal, and C. H. Larsen, "The disign of erbium-doped fiber amplifiers," *J. Lightwave Technol.*, vol. 9, pp. 1105–1112, Sept. 1991.

[16] C. R. Giles and E. Desurvire, "Modeling erbium-doped fiber amplifiers," *J. Lightwave Technol.*, vol. 9, pp. 271–283, Feb. 1991.

[17] M. J. F. Digonnet, "Closed-form expressions for the gain in the three- and four-level laser fibers," *IEEE J. Quantum Electron.*, vol. 26, pp. 1788–1796, Oct. 1990.

[18] C. Barnard, P. Myslinski, J. Chrostowski, and M. Kavehrad, "Analytical model for rare-earth-doped amplifiers and lasers," *IEEE J. Quantum Electron.*, vol. 30, pp. 1817–1830, Aug. 1994.

[19] S. Jarabo and M. A. Rebolledo, "Analytic modeling of erbium-doped fiber amplifiers on the basis of intensity-dependent overlapping factors," *Appl. Opt.*, vol. 34, pp. 6158–6163, Sept. 1995.

[20] R. Oron and A. Hardy, "Approximate analytical expressions for signal amplification in strongly pumped fiber amplifiers," *Inst. Elect. Eng. Proc.—Optoelectron.*, vol. 145, pp. 138–140, Apr. 1998.

[21] C. B. Layne, W. H. Lowdermilk, and M. J. Weber, "Multiphonon relaxation of rare-earth ions in oxide glasses," *Phys. Rev. B*, vol. 16, pp. 10–20, July 1977.

[22] X. Zou and T. Izumitani, "Spectroscopic properties and mechanisms of excited state absorption and energy transfer upconversion for Er^{3+}-doped glasses," *J. Non-Crystalline Sol.*, vol. 162, pp. 68–80, Jan. 1993.

[23] C. Y. Chen, R. R. Petrin, D. C. Yeh, and W. A. Sibley, "Concentration-dependent energy-transfer processes in Er^{3+}- and Tm^{3+}-doped heavy-metal fluoride glass," *Opt. Lett.*, vol. 14, pp. 432–434, May 1989.

[24] K. Shuto, K. Hattori, T. Katigawa, Y. Ohmori, and M. Horiguchi, "Erbium-doped phosphsilicate glass amplifier fabricated by PECVD," *Electron. Lett.*, vol. 29, pp. 139–141, Jan. 1993.

[25] T. Katigawa, K. Hattori, K. Shuto, M. Yasu, M. Kobayashi, and M. Horiguchi, "Amplification in erbium-doped silica-based planar lightwave circuits," *Electron. Lett.*, vol. 28, pp. 1818–1819, Sept. 1992.

[26] F. Di Pasquale and M. Federighi, "Modeling of uniform and pair-induced upconversion mechanism in high-concentration erbium-doped silica waveguides," *J. Lightwave Technol.*, vol. 13, pp. 1858–1864, Sept. 1995.

[27] R. Olshansky, "Propagation in glass optical waveguides," *Rev. Mod. Opt.*, vol. 51, pp. 341–367, Apr. 1979.

[28] F. Ladouceur, J. D. Love, and T. J. Senden, "Measurement of surface roughness in buried channel waveguides," *Electron. Lett.*, vol. 28, pp. 1321–1322, July 1992.

[29] F. P. Payne and J. P. R. Lacey, "A theoretical analysis of scattering loss from planar optical waveguides," *Opt. Quantum Electron.*, vol. 26, pp. 977–986, June 1994.

[30] F. Auzel, "Existence of intrinsic 'backgroud loss' in rare-earth doped fibers: Drawbacks and usefulness," *Electron Lett.*, vol. 29, pp. 337–338, Feb. 1993.

[31] N. Ikegami, Y. Miyakawa, J. Hashimoto, N. Ozawa, and J. Kanamori, "Role of fluorine in reactive ion etching on silicon dioxide," *Jpn. J. Appl. Phys.: Part I*, vol. 32, pp. 6088–6094, Dec. 1993.

[32] T. Yoshimura, H. Shiraishi, J. Yamamoto, and S. Okazaki, "Correlation of nano edge roughness in resist patterns with base polymers," *Jpn. J. Appl. Phys.: Part I*, vol. 32, pp. 6065–6070, Dec. 1993.

[33] K. Hattori, T. Kitagawa, M. Oguma, and H. Okazaki, "Optical amplification in Er^{3+}-doped P_2O_5-SiO_2 planar waveguides," *J. Appl. Phys.*, vol. 80, pp. 5301–5308, Nov. 1996.

[34] J. R. Bonar, M. V. D. Vermelho, P. V. S. Marques, A. J. McLaughlin, and J. S. Aitchison, "Fluorescence lifetime measurements of aerosol doped erbium in phosphosilicate planar waveguides," *Opt. Commun.*, vol. 149, pp. 27–32, Apr. 1998.

M. V. D. Vermelho was born in Bom Sucesso-PR, Brazil, on February 29, 1960. He received the B.S. degree in electrical engineering from the Technological Educational Centre of the State of Parana (CEFET-PR) in 1985 and the M.Phil. degree in physics from the Federal University of Alagoas (UFAL-AL) in 1994 for work carried out on nonlinear propagation of picosecond pulsed in optical fibers. He is currently working towards the Ph.D. degree with the optoelectronic group at the Department of Electronics and Electrical Engineering at University of Glasgow, on optimization of erbium-doped waveguide fabricated by flame hydrolysis method.

From 1985 to 1992, his work was related with electrical engineering, including the installation of 13.8-kV transmission lines. During 1994–1995, he was with the nonlinear optics group at the Physics Department at the Federal University of Alagoas as a Research assistant.

Ulf Peschel was born in 1964. He received the diploma and the Ph.D. degrees in physics from Friedrich-Schiller Universitat, Jena, Germany, in 1990 and 1994, respectively.

From 1990 to 1998, he worked as a Research Assistant at Friedrich-Schiller Universitat. He is currently working at the University of Glasgow. U.K. His main research interests are integrated optics and nonlinear dynamics in optical systems.

J. Stewart Aitchison (M'96) received the degrees of B.Sc. and Ph.D. degrees from The Physics Department, Heriot-Watt University in 1984 and 1987, respectively. His dissertation work was on optical bistability in semiconductor waveguides.

From 1988 to 1990, he was a Postdoctoral Member of Technical Staff with Bellcore, NJ. His research interests were in the areas of highly nonlinear glasses and spatial soliton propagation. He joined The Department of Electronics and Electrical Engineering at The University of Glasgow, U.K., in 1990 as a Lecturer and was promoted to Senior Lecturer in 1995 and Reader in 1998. Since his appointment at The University of Glasgow, he has developed his interests in nonlinear optical waveguides. In particular, III–V semiconductors operated at the half band gap for optical switching and soliton propagation. More recently, his attention has focused on second order effects for all-optical switching and frequency conversion applications. He has also developed research interests in planar silica technology for photosensitivity, waveguide lasers and passive components. In 1996 he was the holder of a Royal Society of Edinburgh Personal Fellowship to carry out research on spatial solitons. He is the author or co-author of over 200 refereed journal and conference papers.

Dr. Aitchison is a member of the Institute of Physics, the Optical Society of America (OSA), and IEEE/LEOS.